2021

Dynamic Modeling of Packaged Air Conditioner with Micro-Channel Heat Exchanger Condenser

Khaled I. Alghamdi
Oklahoma State University, United States of America, khaled.alghamdi@okstate.edu

Christian K. Bach

Dynamic Modeling of Packaged Air Conditioner with Microchannel Heat Exchanger Condenser

Khaled Ibrahim ALGHAMDI[1*], Christian Konrad BACH[2]

[1,2] Oklahoma State University, Mechanical and Aerospace Engineering School,
Stillwater, OK 74074, USA

[1] Contact Information: khaled.alghamdi@ostate.edu
[2] Contact Information: cbach@okstate.edu

* Corresponding Author

ABSTRACT

Microchannel Heat Exchangers (MCHX) are used in Air Conditioning systems (AC) as an efficient type of Heat Exchangers (HX) because they have compact size, as well as low refrigerant charge. However, using MCHX as condensers can be associated with some problems, including evaporator-condenser transient charge balance issues. Therefore, this study aims to investigate the impact of using MCHX as a condenser in a packaged air conditioner with a fin-and-tube heat exchanger as an evaporator. The methodology was dynamically modeling the packaged air conditioner in Modelica, considering varying pass configurations of MCHX with several refrigerant charges. The results showed that the pressure in the high-pressure side of the refrigerant cycle increases as the number of tubes in the inlet-pass of the MCHX decreases. In addition, if the difference in the number of tubes among the inlet-pass and the outlet-pass is large, the pressure increases regardless of which pass has the highest number of tubes. Moreover, the pressure can increase after a while at the beginning of an on-cycle due to the slow response of Thermostatic Expansion Valve (TXV) caused by the thermal inertia of the sensing bulb. We defined a mass ratio as mass of refrigerant in the evaporator to the mass in the condenser. A decrease in the mass ratio for a given total charge corresponds to the refrigerant accumulating in the condenser, increasing pressure in the condenser.

1. INTRODUCTION

Heat exchangers (HX) are key components in Air Conditioning systems (AC), as they are the medium where the AC's main function, which is to transfer heat, takes a place. Improving HX performance can positively impact the overall performance of AC, as it decreases equipment's pressure ratio. In the context of improving HXs, Microchannel Heat Exchangers (MCHX) have been introduced as an efficient alternative to other heat exchanger types, such as fin-and-tube heat exchangers. With compact sizes and less refrigerant charges, MCHX can maintain the same capacity provided by other types of HXs (Yun et al., 2006). However, use of MCHX might cause some problems, such as accumulation of refrigerant at the condenser if MCHX are used as condensers (Li et al., 2017).

To investigate parameters causing problems associated with using MCHX, simulations can be an effective approach. Indeed, designing and optimizing HX based on simulations is an effective tool because such a tool requires fewer resources as compared to other designing methods (Tao Ren & Hu, 2013). In terms of modeling HX generally, Aute (2016) provided a literature review. In terms of particular models of MCHX, Pfafferott & Schmitz (2004) developed a model for MCHX to enhance a library of CO_2 refrigerant systems. The model was developed in Modelica using the connectors feature, which allows defining the interactions among several components. Hu et al. (2011) developed a dynamic model of MCHX. They utilized EASY5, which is a software for dynamic simulation (MSC.Software, 2019), as a tool for simulating and controlling the MCHX model. In addition, Li et al. (2017) studied the maldistribution of refrigerant flow in MCHX at the port level. They developed a MCHX model considering varying operation conditions to observe their impacts on causing maldistribution. Also, Huang et al. (2014) developed a model considering several geometries of MCHX for steady-state and fully-developed flows.

However, the mentioned literature lacks examples of use of dynamic models of MCHX as it is used within a system as a condenser with a fin-and-tube evaporator. Hence, the aim of this study is to model a MCHX condenser in a packaged air conditioner with a fin-and-tube evaporator to investigate the impact of using the MCHX on the behavior of the air conditioner at dynamic and steady-state conditions. In this paper, Section 2 explains the development process of modeling the air conditioner, Section 3 reviews the simulation setup, Section 4 represents and discusses the results obtained from simulating the model, and Section 5 concludes this study.

2. MODEL DEVELOPMENT

The packaged air conditioner in this study was assumed to have the four basic components of a vapor-compression cycle: compressor, condenser, expansion valve, and evaporator. In addition, since the model of this study was used to investigate dynamic issues associating with using MCHX, Modelica was selected as the modeling language with Dymola 2020 as an environment for Modelica. Modelica is a high-level programming language for representing systems' behaviors (Tiller, 2019). Modelica has various libraries containing components to be used in modeling systems. Among the libraries, TIL Suite 3.7.0, which was developed by TLK-Thermo Gmbh, was selected because the library includes a model of MCHX: Multiple Port Extruded Tubes (MPET). The TIL library was developed for dynamic and steady simulations of thermal systems (TLK-Thermo GmbH, 2019b). In addition, TIL library integrates TILMedia Suite, which is a library for calculating thermophysical properties of various fluids (TLK-Thermo GmbH, 2019a). Additionally, the connectors feature in Modelica, which allows to define the interactions among components (Pfafferott & Schmitz, 2004), was used to connect the components with each other. The components were modeled as specified in the the following subsections.

2.1 Ideal AC Cycle

Prior to model the components in Modelica, an ideal AC cycle was modeled in Engineering Equation Solver (EES). EES is a software for solving non-linear equations, and it has the capability to solve problems involving thermodynamic and transport properties (F-Chart Software, 2019). The outputs of the EES model were used for initialization of the components in Modelica. Table 1 shows the inputs and outputs of the EES model. The temperature values in the inputs were assumed based on the temperature difference between air outlet and refrigerant at the evaporator by 7°C, and at the condenser by 5°C. For the air temperature conditions, they were considered in accordance with test A in Table 8 of AHRI Standard 210/240 (AHRI, 2017) for the condenser, and supply conditions of 15 °C for the evaporator. Refrigerant R410A was used as the working fluid throughout this study. The air conditioner was assumed to have a nominal capacity of 7 tons of cooling (24.6 kW). The compressor was assumed to have 100% isentropic efficiency, and the enthalpy through the expansion valve was constant.

Table 1: Inputs and outputs of the AC cycle modeled in EES with R410A as a refrigerant.

State	Temperature (T) [°C]	Vapor Quality (x)	Pressure [kPa]	Enthalpy [kJ/kg]	Entropy [$kJ/kg \cdot K$]	Note
Compressor in	7	1	991.8	423.3	1.797	x is an input
Condenser in	40	Superheat	1889	440.5	1.797	T is an input
Expansion valve in	30	0	1889	248.3	1.164	x is an input
Evaporator in	7	0.1765	991.8	248.3	1.172	T is an input

2.2 Condenser

Since the objective of this study is to model an air conditioner with MCHX condenser, the MPET model of Moist Air to Vapor-Liquid-Equilibrium Fluid (MoistAirVLEFluid) of the TIL library was selected. The flow configuration of the condenser was cross-flow, which means the air flow was perpendicular to the refrigerant flow. The geometric specifications of the condenser were introduced to the MPET model in accordance with the specifications shown in Table 2a. In addition, the initialized parameters for the MCHX model were set in accordance with the results obtained from the EES model, which is shown in Table 1.

2.3 Evaporator

For the evaporator, a model of fin-and-tube was selected from TIL library; in particular, it was the FinAndTube model of MoistAirVLEFluid. The flow configuration of the evaporator was cross-flow. The geometric specifications of the evaporator model were set as as shown in Table 2b. As with the condenser, the initialized parameters were set in accordance with the results shown in Table 1.

Table 2: Condenser and evaporator specifications.

(a) Condenser specifications.

Parameter	Value
MCHX width	132.4 cm
MCHX height	63.9 cm
MCHX depth	2.5 cm
Tube thickness	1.3 mm
Fin pitch	1.1 mm
Manifold diameter	3.2 cm
Overall volume	1.667 L
Number of Passes	2 passes
Number of tubes [per Pass]	65 [35,30] tubes
Number of ports per tube	26 ports
Manifold cross-section area	8.1 cm^2
Manifold volume	1.028 L
Ports volume	0.639 L
Port length	126 cm
Cross-section area of port	0.3 mm^2
Diameter of port	0.6 mm
Perimeter of port	2.5 mm

(b) Evaporator specifications.

Parameter	Value
Length of finned tubes	88.9 cm
Width of finned tubes	88.9 cm
Thickness of finned tubes	13.2 cm
Number of serial tubes	6 tubes
Number of parallel tubes	35 tubes
Diameter of tube	1.0 cm
Fin thickness	0.15 mm
Distance between fins	2 mm
Thickness of wall	0.30 mm
Number of circuits	15 circuits
Number of tubes per circuit	14 tubes
Distance between parallel tubes	1.6 cm
Distance between serial tubes	1.6 cm

2.4 Expansion Valve

From TIL library, a model of Thermostatic Expansion Valve (TXV) was used. According to the documentation of the model, the TXV model requires defining two curves: the opening curve and the flow rate curve. The opening curve governs the relationship between outlet pressure and temperature of the evaporator. The opening curve is characterized by 3 reference points. Three reference points are essential as the curve has two different parts: exponential and linear. The exponential part is determined by Equation (1), and the linear part is determined by Equation (2).

$$P_{open} = \exp(B - (A/T_{evap,out})) \tag{1}$$

$$P_{open} = C \cdot T_{evap,out} + D \tag{2}$$

By introducing reference points into Equation (1) and Equation (2), the parameters, A, B, C, and D, can be determined. Then, the parameters can be used in determining an opening curve for other pressure and temperature points. The point where the curve changes from exponential into linear is determined by either Maximum Operation Temperature (MOT) or Maximum Operation Pressure (POT). For the opening curve in the TXV model, the model takes inputs of the reference points, as well as MOT or POT.

For the flow rate curve, the TXV model characterizes the curve by nominal pressure, high ($P_{nom,high}$) and low ($P_{nom,low}$), of the refrigerant cycle, nominal evaporator outlet temperature ($T_{evapout,nom}$), nominal refrigerant flow rate (m_{nom}), maximum refrigerant flow rate (m_{max}), and curvature exponent (n). Equations (3)-(7) determine the flow rate curve.

$$A_{nom} = m_{nom}(2 \cdot \rho_{nom}(P_{high,nom} - P_{low,nom})) \tag{3}$$

$$A_{max} = m_{max}(2 \cdot \rho_{nom}(P_{high,nom} - P_{low,nom})) \tag{4}$$

$$\beta = \frac{A_{nom}}{(P_{high,nom} - P_{low,nom})} \tag{5}$$

$$A_{eff,lin} = \beta \cdot (P_{open} - P_{evapout,nom}) \tag{6}$$

$$A_{eff} = A_{eff,lin} + A_{max} - (A_{eff,lin}^{n} - A_{max}^{n})^{1/n} \tag{7}$$

Where, $A_{eff,lin}$ is the linear effective flow area through the valve, A_{eff} is the effective flow area, A_{max} is the maximum flow area, ρ_{nom} is the density of saturated vapor at $P_{nom,high}$, and $P_{open,nom}$ is the pressure value at $T_{evapout,nom}$ from the opening curve.

To plot the opening curve, a code was developed in EES. The code takes three reference points as inputs and returns the opening curve. In addition, the dew curve, which shows the two-phase region and the gas region, for R410A was plotted. Figure 1 shows the opening curve of TXV with specifications listed in Table 3, as well as the dew curve of R410A. The values in Table 3 was entered in the TXV model used in this study.

Table 3: The inputs of the TXV model of this study.

Parameter	**Value**
1^{st} T_{ref} point	0°C
1^{st} P_{ref} point	4 bar (400 kPa)
2^{nd} T_{ref} point	10°C
2^{nd} P_{ref} point	7 bar (700 kPa)
3^{rd} T_{ref} point	40°C
3^{rd} P_{ref} point	20 bar (2000 kPa)
Maximum Operation Temperature (MOT)	25°C
Time constant	60 seconds

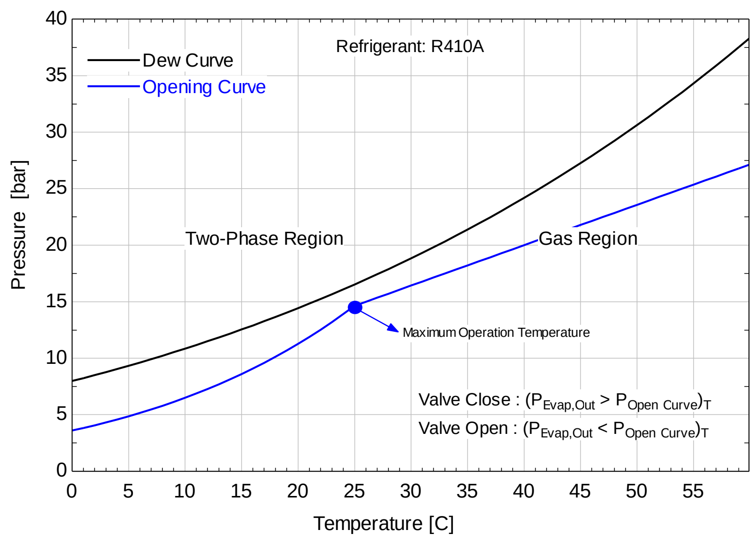

Figure 1: The opening curve of the TXV specified in Table 3, as well as the dew point curve of R410A.

2.5 Compressor

For the compressor, an efficiency compressor model in TIL library was used. The model has a name of effCompressor, and its inputs are shown in Table 4.

3. SIMULATION SETUP

The components mentioned in Section 2 were connected in a cycle, as illustrated in Figure 2, to form the model of the air conditioner. Then, the model was simulated in accordance with the simulation plan shown in Table 5.

Table 4: Inputs of the compressor model used in this study.

Parameter	Values
Speed	60 Hz
Displacement	6E-5 m^3
Volumetric efficiency	70%
Isentropic efficiency	70%
Effective isentropic efficiency	70%

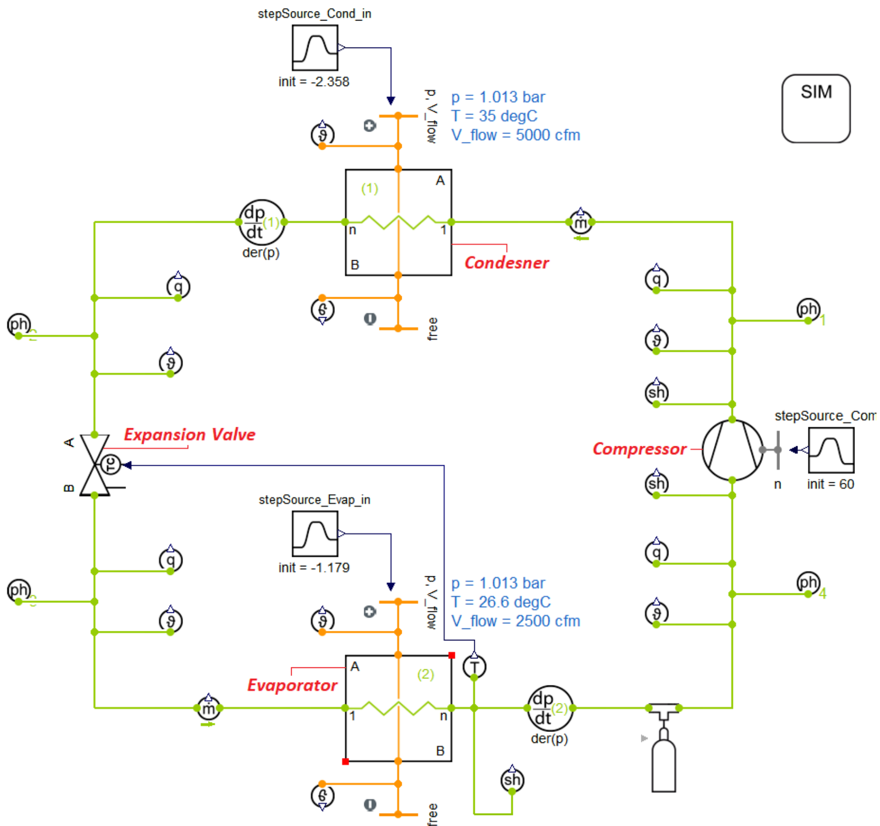

Figure 2: The model schematic diagram.

For the refrigerant charge, the model gave unreasonable results whenever the value exceeded 1.5 kg. Also, to have control over the amount of the refrigerant charge, a filling station model was added to the cycle. The filling station model allows to specify the amount of charge, as well as the maximum flow rate of the charging process. The simulation started with an initial refrigerant mass in the cycle itself.

Moreover, the impact of cycling, vary between 'on' and 'off', on the performance of the air conditioner was considered to be observed through modeling three cycles, each of which had a different duration. The cycles were modeled by adding source models depending on time to the compressor speed and volumetric flow rate at the air-inlet of the evaporator and the condenser.

For the air input data, the temperature values were set in accordance with Test A in Table 8 of AHRI Standard 210/240 (AHRI, 2017), while the volumetric flow rate was set in accordance with 350 cfm/ton for the evaporator and 700 cfm/ton for the condenser. Hence, since the capacity of the air conditioner was considered to be 7-ton of cooling, the volumetric flow rate of the air at the inlet of the evaporator was 2,500 cfm (1.179 m^3/s) and 5,000 cfm (2.359 m^3/s) at the air inlet of the condenser.

For the number of passes of MCHX and their configurations, they were considered in our parametric study with several

Table 5: The simulation plan of this study.

Parameter	Value		
Simulation time	60 minutes		
Interval length	0.1 seconds		
Integration algorithm and tolerance	Dassl with tolerance of 0.0001		
Refrigerant charge	1.2, 1.5, or 2 kg (2.64, 3.3, and 4.4 lb.)		
Refrigerant charge flow rate	0.01 kg/s (0.022 lb./s)		
On-off cycles	1^{st} cycle: 10 minutes 'on' then 10 minutes 'off' 2^{nd} cycle: 10 minutes 'on' then 20 minutes 'off' 3^{rd} cycle: 10 minutes 'on'		
Condenser	Air inlet temperature	35°C (95°F)	
	Air inlet humidity	100%	
	Air inlet flow rate	2.358 m^3/s (5,000 cfm)	
	Heat transfer model	Constant $\alpha = 1000 W/m^2 \cdot K$	
	Pressure drop model	Swamee-Jain Correlation	
	Number of passes	2	3
	Number of tubes/pass	[15,50]	[15,20,30]
		[25,40]	[25,20,20]
		[30,35]	[30,20,15]
		[35,30]	[15,25,25]
		[40,25]	[20,25,20]
		[50,15]	[25,25,15]
Evaporator	Air inlet temperature	26.6°C (80°F)	
	Air inlet humidity	50%	
	Air outlet temperature	15°C (59°F)	
	Air outlet humidity	90%	
	Air inlet flow rate	1.179 m^3/s (2,500 cfm)	
	Heat Transfer Model	Constant $\alpha = 500 W/m^2 \cdot K$	
	Pressure drop model	Swamee-Jain correlation	

values to observe their impact on the performance of the air conditioner. Constant heat transfer coefficient, α, was selected as a heat transfer model at the refrigerant side. α was assumed, as shown in Table 5, based on reviewing such a value in model examples in TIL library for the same component type.

4. RESULTS AND DISCUSSION

After the model of the air conditioner had been developed as specified in Section 2, the model was simulated in accordance with the simulation plan described in Table 5.

In terms of the pressure in the high-pressure side of the cycle, which is at the condenser side, the discharge pressure of the compressor is the reference throughout this section. Generally, the pressure increased as the number of tubes in the inlet-pass decreased, as Figure 3a - 3b and Figure 4a - 4b show for the case of the 2^{nd} on-cycle of 1.2 kg and 1.5 kg refrigerant charge, respectively. The decrease of tubes in the inlet-pass means an increase in the number of tubes in the outlet-pass.

To find an explanation for such a pattern, the refrigerant vapor-quality was observed at the end of the inlet-pass. For vapor-quality with 1.2 kg of refrigerant charge, the quality was lower at the end of the inlet-pass for the pass configurations with a high number of tubes in that pass. The high number of tubes enhance the heat transfer process as surface area increases. As a result, the condensation of the refrigerant is higher with such configurations than other configurations with the lower number of tubes in the inlet-pass. With low vapor-quality, the volume of the refrigerant passing to the outlet-pass is less, so a low number of tubes might not affect the refrigerant flow to a degree where it starts accumulating. However, with 1.5 kg of refrigerant charge, the refrigerant has already been condensed at the end of the inlet-pass in most of the pass configurations, yet the density of the refrigerant was not the same. The density increased as the number of tubes in the inlet-pass increased. The refrigerant had less volume at the end of the inlet-pass with pass configurations of more tubes in the inlet-pass. Hence, the same explanation with a refrigerant charge of 1.2 kg can be applied with the refrigerant charge of 1.5 kg.

In addition, the 2-pass configuration of 50 and 15 tubes for the inlet- and outlet-pass, respectively, as well as the 3-pass configuration of 30, 20, and 15 tubes for the inlet-, middle-, and outlet-pass, respectively, were outliers in terms of pressure. Despite they had a high number of tubes in the inlet-pass, the pressure increased. These configurations have relatively a low number of tubes in the outlet-pass to a point the refrigerant flow might be affected, which results in a pressure increase to maintain the continuity.

In terms of the effect of cycling on the pressure in the refrigerant-side of the air conditioner, the 1^{st} on-cycle experienced a sharp increase in the pressure around the same time, which is 5 seconds from the beginning of the cycle, for all configurations. Observing the mass ratio of the refrigerant in the evaporator to that in the condenser, the mass ratio was the minimum, with a value of 0.5 for all configurations, at the same time where the pressure increased sharply, as Figure 6 shows. The simulation started with an initial refrigerant mass, which was identical in all cases, so all configurations had identical mass ratio by that time. The increase in the mass ratio indicated the refrigerant was accumulating in the condenser. As the refrigerant was accumulating in the condenser while the expansion valve was closed, as reviewing the simulation data revealed, the pressure increased dramatically then decreased, as the valve opened. For the 2^{nd} and 3^{rd} on-cycles, the pressure was almost identical in terms of values and patterns. Observing the same pressure values and patterns in both cycles means the duration of the off-period might not have a significant impact on the refrigerant pressure.

In the 2^{nd} and 3^{rd} cycle, the pressure increased around a minute after the cycles began. The increase in the pressure occurred despite the compressor was running at a constant speed. After reviewing the flow area of the expansion valve, it was found that the flow area did not change at the beginning of the cycles; it was changed at the same time when the pressure increased. Therefore, the pressure increased due to a decrease in the flow area of the expansion valve. The delay could be caused by the thermal inertia of the expansion valve, as the model requires a time constant to determine the effect of the thermal inertia on the performance of TXV. However, the value of the time constant was set as the default value suggests, which is 60 seconds. Also, to increase the response time of the expansion valve, the time constant was decreased, yet the mass flow rate showed high fluctuation due to sensitivity of the valve, so the time constant was returned to its default value.

For the case of 2.0 kg of refrigerant charge, as shown in Figure 5a - 5b, the pressure increased dramatically in all pass configurations; the simulations were terminated, for instance, at the beginning of the 2^{nd} on-cycle of the case of the 3-pass configurations.

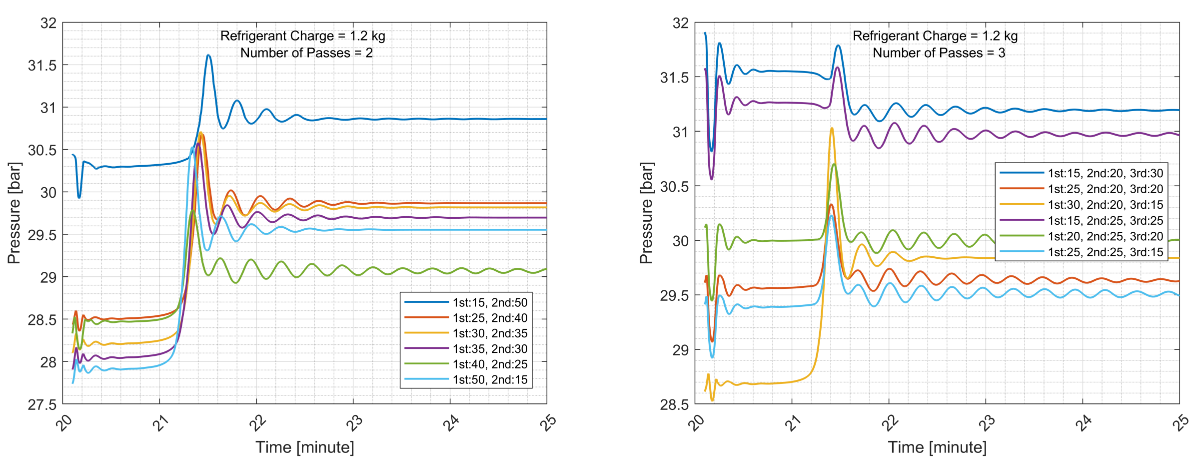

(a) 2-pass configuration (legend - pass no.: no. of tubes) **(b)** 3-pass configuration (legend - pass no.: no. of tubes)

Figure 3: Pressure at the high-pressure side of the cycle in the beginning of the 2^{nd} on-cycle: 1.2 kg refrigerant charge.

In terms of refrigerant mass distribution among the condenser and evaporator for the same pass configuration and

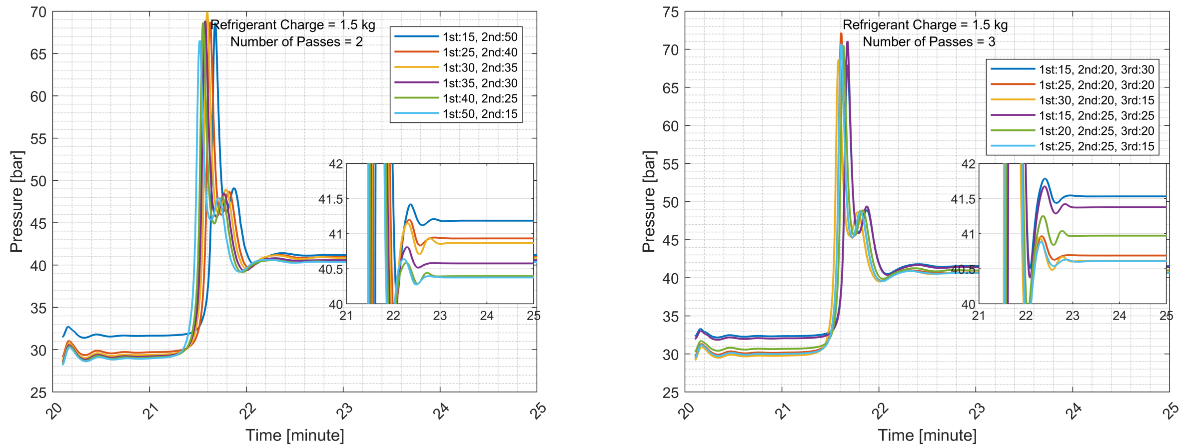

(a) 2-pass configuration (legend - pass no.: no. of tubes)

(b) 3-pass configuration (legend - pass no.: no. of tubes)

Figure 4: Pressure at the high-pressure side of the cycle in the beginning of the 2^{nd} on-cycle: 1.5 kg refrigerant charge.

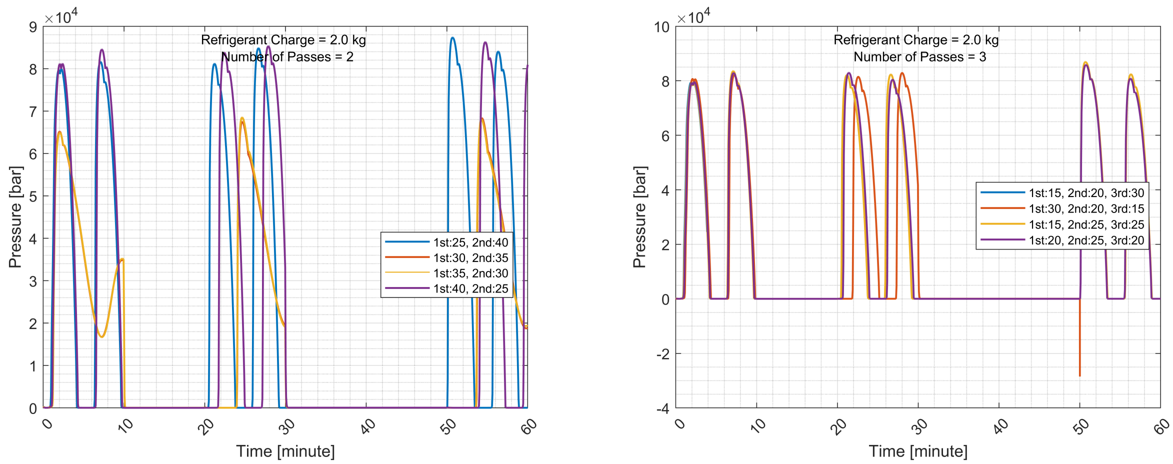

(a) 2-pass configuration (legend - pass no.: no. of tubes)

(b) 3-pass configuration (legend - pass no.: no. of tubes)

Figure 5: Pressure at the high-pressure side of the cycle for the entire simulation duration: 2.0 kg refrigerant charge.

refrigerant charge, the mass ratios in all tube configurations were close except in the case of 1.2 kg of refrigerant charge with the configurations of 40 and 25 tubes in the inlet- and outlet-pass, respectively, for the 2-pass configuration, and of 30, 20, and 15 tubes in inlet-, middle-, and outlet-pass , respectively, for the 3-pass configuration. For the mass ratio comparison among different refrigerant charges, the mass ratio was higher in 1.2 kg refrigerant charge than that of the case of 1.5 kg refrigerant charge. For the effect of the pass configuration, 2-pass or 3-pass, on the mass ratio, the pass configuration had no effect in the case of 1.5 kg refrigerant charge, while the ratio was high with 3-pass configuration as compared to 2-pass configuration in the case of 1.2 kg refrigerant charge.

5. CONCLUSION

The impact of using MCHX condenser in a packaged air conditioner with a fin-and-tube evaporator was investigated in this study. The air conditioner was modeled in Modelica with varying pass configurations, as well as refrigerant charge, in order to observe their effect on the transient system behavior. At the refrigerant-side, the pressure in the high-pressure side increases as the number of tubes in the inlet-pass decreases. Nevertheless, if the difference in the number of tubes in the inlet-pass to those in the outlet-pass is high, the pressure increases regardless of the inlet-pass or outlet-pass has the higher number of tubes. The duration of an off-cycle had no impact on the pressure. Also, the

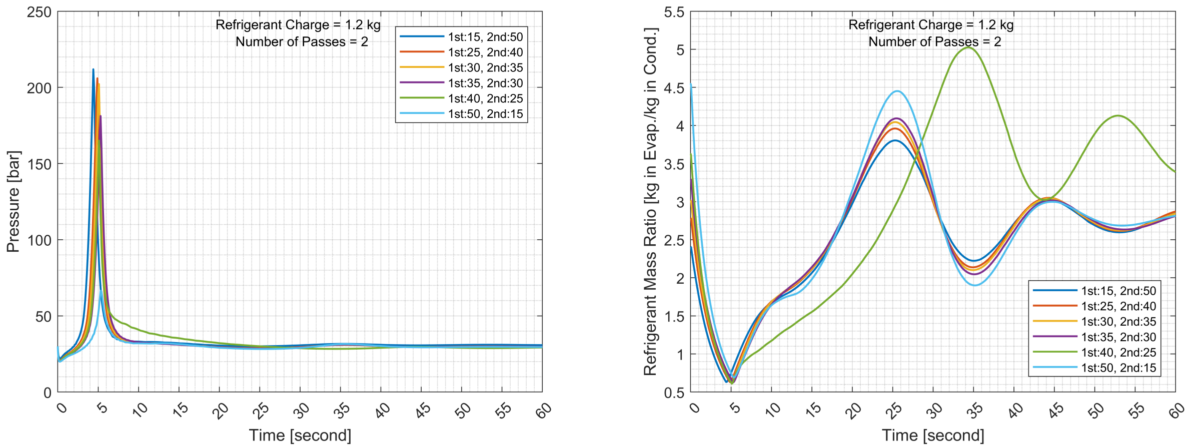

(a) Refrigerant pressure (legend - pass no.: no. of tubes) **(b)** Refrigerant mass ratio (legend - pass no.: no. of tubes)

Figure 6: Illustration of the refrigerant accumulation in the condenser and its impact on the refrigerant pressure at the high-pressure side of the refrigerant cycle.

pressure can increase after a while, which in this study was around a minute as the time constant of the TXV model was set to a minute, of the start of an on-cycle due to thermal inertia of TXV. In terms of the mass of refrigerant, the pressure increases as the ratio of the mass in the evaporator to that in the condenser decreases, which means the refrigerant starts accumulating in the condenser. Finally, several assumptions for modeling some of the components were made. Future work should include selection and detailed model adjustments of a specific unit, as well as experimental validation of the capabilities of the model.

NOMENCLATURE

AC	Air Conditioning system	
EES	Engineering Equation Solver	
HX	Heat Exchanger	
MCHX	Microchannel Heat Exchanger	
MOP	Maximum Operation Pressure	
MOT	Maximum Operation Temperature	
TXV	Thermostatic Expansion Valve	
A	Area	m^2
cfm	Cubic Feet per Minute	ft^3/min
m	Mass flowrate	kg/s
P	Pressure	kPa
T	Temperature	$°C$
ρ	Density	kg/m^3

Subscript

evap	Evaporator
cond	Condenser
refg	Refrigerant
nom	Nominal
eff	Effective
lin	Linear

REFERENCES

AHRI. (2017). *AHRI Standard 210/240 - Standard for Performance Rating of Unitary Air-conditioning & Air-source Heat Pump Equipment.* Air-Conditioning, Heating, & Refrigeration Institute, [Online: Accessed 11-27-2019]. Available from: `http://www.ahrinet.org/App_Content/ahri/files/STANDARDS/AHRI/AHRI_Standard_210-240_2017.pdf`.

Aute, V. C. (2016). A review of state of the art in modeling of air-to-refrigerant heat exchangers for hvac&r applications. In *Proceedings of International Refrigeration and Air Conditioning Conference at Purdue* (pp. 2543-1 – 2534-10). Indina, USA.

F-Chart Software. (2019). *EES Overview.* [Online: Accessed 11-30-2019]. Available from: `http://fchartsoftware.com/ees/`.

Hu, Y., Su, J., & Yan, Z. (2011). The application of EASY5 software to simulate the operating characteristics of parallel-flow condensing unit. *Procedia Engineering*, *12*, 133–140.

Huang, L., Aute, V., & Radermacher, R. (2014). A model for air-to-refrigerant microchannel condensers with variable tube and fin geometries. *International Journal of Refrigeration*, *40*, 269–281.

Li, Z., Ling, J., Aute, V., & Radermacher, R. (2017). Investigation of port level refrigerant flow maldistribution in microchannel heat exchanger. In *Proceedings of 12th IEA Heat Pump Conference at Rotterdam.* Netherlands.

MSC.Software. (2019). *Product Datasheet - Easy5^{TM}*. [Online: Accessed 12-04-2019]. Available from: `https://www.mscsoftware.com/Submitted-Content/Resources/ds_easy5_ltr_0.pdf`.

Pfafferott, T., & Schmitz, G. (2004). Modelling and transient simulation of CO_2-refrigeration systems with modelica. *International Journal of Refrigeration*, *27*(1), 42–52.

Tao Ren, T. W., Guoliang Ding, & Hu, H. (2013). A general three-dimensional simulation approach for micro-channel heat exchanger based on graph theory. *Applied Thermal Engineering*, *59*(1-2), 660–674.

Tiller, M. M. (2019). *Modelica by example* (0.6.0 ed.). Self-published.

TLK-Thermo GmbH. (2019a). *TILMedia Suite – Software package for calculating the properties of thermophysical substances.* [Online: Accessed 11-30-2019]. Available from: `https://www.tlk-thermo.com/index.php/en/software/tilmedia-suite`.

TLK-Thermo GmbH. (2019b). *TIL Suite – Simulates thermal systems.* [Online: Accessed 11-27-2019]. Available from: `https://www.tlk-thermo.com/index.php/en/software/til-suite`.

Yun, R., Hwang, Y., Radermacher, R., & Zecirovic, R. (2006). Comparison of performance of a residential air-conditioning system using microchannel and fin-and-tube heat exchanger. In *Proceedings of International Refrigeration and Air Conditioning Conference at Purdue* (pp. R108-1 – R108-8). Indina, USA.